Journal of Alloys and Compounds 509S (2011) S732–S735

Contents lists available at ScienceDirect

Journal of Alloys and Compounds

journal homepage: www.elsevier.com/locate/jallcom

$Li_{3-x}M_xN$ (M = Co, Ni) synthesized by Spark Plasma Sintering for hydrogen storage

Junxian Zhang[a,*], Radovan Černý[b], Benjamin Villeroy[a], Claude Godart[a], Dhanesh Chandra[c], Michel Latroche[a]

[a] *Chimie Métallurgie des Terres Rares, ICMPE-UMR 7182, CNRS, 2-8 rue Henri Dunant, 94320 Thiais, France*
[b] *Laboratory of Crystallography, University of Geneva, 24 quai Ernest-Ansermet, Geneva, Switzerland*
[c] *University of Nevada, Reno, USA*

ARTICLE INFO

Article history:
Received 13 July 2010
Received in revised form 8 September 2010
Accepted 26 September 2010
Available online 2 October 2010

Keywords:
Hydrogen storage
Lithium nitride
SPS synthesis
Crystal structure

ABSTRACT

Lithium nitride has recently emerged as a promising material for hydrogen storage. The hydrogen storage capacity reaches 10.2 wt% H by the formation of compounds, such as imides, amides, and others. Hydrogenation of lithium nitride is highly exothermic, and thus desorbing hydrogen from these compounds requires high temperature and cannot be used for reversible hydrogen storage. *Ab initio* calculations predict that partial substitution of Li by transition metals like Cu or Ni can reduce the reaction enthalpy between amide and imide. In this work, we present the synthesis of the ternary system $Li_{3-x}M_xN$ (M = Co or Ni) by Spark Plasma Sintering (SPS). The samples are hydrogenated at 255 °C by solid gas reaction. The sample crystal structures have been analyzed by synchrotron X-ray powder diffraction using a high resolution powder diffractometer. The structural models for Co and Ni-substituted Li_3N have been confirmed. The effect of the substitution on the phase formation upon hydrogenation has been investigated at various metal and hydrogen concentration. Different behaviors are observed depending on the nature of M.

1. Introduction

The reaction of Li_3N with H_2 was already reported in the early part of the last century [1]. However, interest in Li_3N as a hydrogen storage materials only began recently when Chen et al. [2] investigated its reversible hydrogen uptake. Lithium nitride has a high theoretical hydrogen uptake capacity of 10.2 wt% via the two following reactions:

$$Li_3N + H_2 \rightarrow Li_2NH + LiH \quad \Delta H = -116\,\text{kJ mol}^{-1}H_2 \tag{1}$$

$$Li_2NH + H_2 \rightarrow LiNH_2 + LiH \quad \Delta H = -66\,\text{kJ mol}^{-1}H_2 \tag{2}$$

The enthalpy of the first reaction is highly exothermic and thus requires very high temperature to release hydrogen [3–6]. Due to incomplete dehydrogenation at a temperature of 255 °C only ~5.8 wt% reversible hydrogen capacity can be obtained. Although one can enhance dehydrogenation by increasing the temperature, some authors demonstrate that dehydrogenation of hydrogenated Li_3N at a temperature of 400 °C is followed by a very low (0.4 wt%) rehydrogenation capacity [7]. *Ab initio* calculations show that partial substitution of Li by transition metals like Cu or Ni can reduce the reaction enthalpy between amide and imide [8]. The ternary Li nitrides $Li_{3-x}M_xN$ (M = Ni, Co, Cu) have been studied for electrochemical applications [9–14] or hydrogen storage [15]. These works have shown that the ternary compound crystallize in a structure isotypic to the parent compound, α-Li_3N, in which the M atoms partially replace Li(1*b*) at the interlayer site and create Li vacancies within the [Li(2*c*)N(1*a*)] planes (Fig. 1).

Recently, studies have shown that non-stoichiometric compound like $Li_{2-x}NH_{1+x}$ and other compounds such as Li_4NH do exist but the thermodynamic properties are not fully established [16–18]. In addition, it is difficult to desorb all the hydrogen during phase transitions:

$$LiNH_2 \rightarrow Li_{2-x}NH_{1-x} \rightarrow Li_2NH \rightarrow Li_4NH \rightarrow Li_3N \tag{3}$$

In particular destabilization of Li_2NH phase is very difficult. For this purpose ternary compounds $Li_{3-x}M_xN$ (M = Co or Ni) have been synthesized using the Spark Plasma Sintering (SPS) technique. It should be noted that simple ball milling of mixed phases does not yield solid solution $Li_{3-x}M_xN$ phase. In addition to preparing the solid solution Li_3N with Co, Ni, we hydrogenated the $Li_{3-x}M_xN$ (M = Co, Ni) solid solutions with two H concentrations, so as to form the expected Li_4NH and $Li_3N_2H_3$ phases. The phase composition and the crystal structure have been studied by synchrotron X-ray diffraction. The influence of the substitution on the crystal structure and hydrogenation properties is discussed.

---

[*] Corresponding author. Tel.: +33 1 4978 1342.
E-mail address: junxian@icmpe.cnrs.fr (J. Zhang).

0925-8388/$ – see front matter © 2010 Elsevier B.V. All rights reserved.
doi:10.1016/j.jallcom.2010.09.160

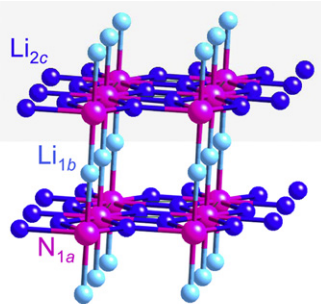

Fig. 1. Crystal structure of α-Li3N (*P*6/*mmm* space group; *a* = 3.647(1) Å, *c* = 3.874(1) Å; N 1*a* (0,0,0); Li 1*b* (0,0,1/2); Li 2*c* (1/3,2/3,0)).

2. Experimental

Solid solution $Li_{3-x}M_xN$ (*M* = Co, Ni) compounds were prepared using the SPS technique from two precursors: Li_3N (Aldrich) and *M* metal powders. First the Li_3N and *M* powders were ball milled together in a Fritsch Pulverisette 7 for 1 h at a rotation speed of 500 rpm with a ball-to-powder mass ratio 10:1. The mixture was sintered by SPS under 50 MPa of pressure for 15 min at 700 °C under Argon partial pressure in a graphite crucible. Then, the samples have been hydrogenated at 255 °C by solid gas reaction at two different hydrogen contents. The first one at $0.7H/Li_3N$ (labeled "a" in Fig. 2) where the Li_4NH phase should form and the second one at 1.4 H/Li_3N (labeled "b" in Fig. 2) where the $Li_3N_2H_3$ phase should occur. Hydrogenated samples have been sealed in glass capillary in a glove box filled with argon and analyzed by synchrotron X-ray powder diffraction at room temperature. The data were collected at the Swiss-Norwegian Beamline (SNBL) at the European Synchrotron Radiation Facility (ESRF) in Grenoble, France, using a high resolution powder diffractometer equipped with a multi-crystal analyzer (λ = 0.50195 Å). Phase analysis and structural determination were done using the full profile fitting program FULLPROF based on the Rietveld's method [19].

3. Results and discussion

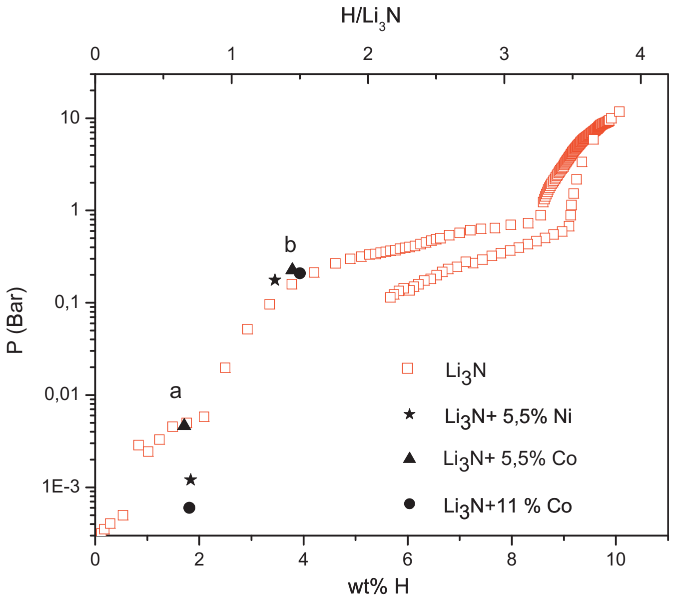

Fig. 2. The pressure–composition isotherm of Li_3N and the hydrogenated points (a at $0.7H/Li_3N$ and b at $1.4H/Li_3N$) for the samples at 255 °C.

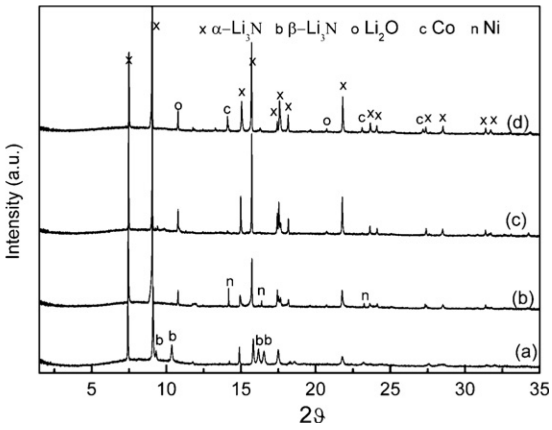

Fig. 3. Synchrotron powder X-ray diffraction patterns of commercial Li_3N (a) and SPS synthesized $Li_{2.95}Ni_{0.05}N$ (b), $Li_{2.95}Co_{0.05}N$ (c) and $Li_{2.89}Co_{0.11}N$ (d) compounds.

The synthesized powders Li_3N + 5%Ni, Li_3N + 5%Co and Li_3N + 11%Co (except precision, the nominal composition $Li_{2.95}Ni_{0.05}N$, $Li_{2.95}Ni_{0.05}N$ and $Li_{2.95}Ni_{0.05}N$ will be used) were compared to as procured Li_3N powders that contained both the α- and β-phases. Powder X-ray diffraction pattern in Fig. 3(a) shows α- and β-Li_3N phases. The α-Li_3N phase crystallizes in the *P*6/*mmm* space group with lattice parameters *a* = 3.647(1) Å, *c* = 3.874(1) Å. It adopts a layered structure with [Li(2*c*)N(1*a*)] planes (where each N is surrounded by a graphitic-like hexagon of six Li atoms) interconnected by Li(1*b*) atoms between layers (Fig. 1). The β-Li_3N phase which is a high pressure phase, crystallizes in $P6_3/mmc$ space group with lattice parameters *a* = 3.552 Å, *c* = 6.311 Å. After the SPS treatment, samples contain only the α-Li_3N-type phase, a small amount of lithium oxide and in some cases, traces of the metal *M*. During SPS processing, the β-Li_3N phase transforms to the α-Li_3N-type and consequently the β-Li_3N phase in not observed in the synthesized materials. Comparing the XRD patterns in Fig. 3(b) and (c) we find the solubility of Ni is less than of Co in α-Li_3N, as residual metallic Ni phase is present as shown in Fig. 3(b). The compound $Li_{2.95}Co_{0.05}N$ shows the maximum solubility and excess Co is present in the compound $Li_{2.89}Co_{0.11}N$; thus there is slightly more solubility of Co than Ni in the α-Li_3N, as suggested by the presence of Bragg peaks of metallic Co in Fig. 3(d). The substitution of lithium by transition metal atoms (Ni or Co) leads to a modification of the cell parameters of α-Li_3N, *a* increases and *c* decreases. This cell evolution indicates a solid solution behavior. The Rietveld refinement shows that Ni or Co replaces partially the Li atoms in the interlayer Li site and additionally creates Li^+ vacancies within the $[Li_2N]$ planes. These results are in agreement with previous studies, the compositions determined by Rietveld analysis are given in Table 1. Traces of pure metal *M* are attributed to an incomplete reaction. The presence of lithium oxide is related to the formation of free lithium during the synthesis following Eq. (4).

$$Li_3N + xM \rightarrow Li_{3-x-y}M_xN + (x + y)Li \tag{4}$$

where *y* stands for the number of created Li vacancies, and the value are 0.47 for *M* = Ni and 0.4 for *M* = Co respectively. Free Li metal that is very reactive may then react with the remaining O_2 gas present in the SPS chamber.

In Fig. 2, the hydrogenation data points for (a) $0.7H/Li_3N$ and (b) $1.4H/Li_3N$ for all the three SPS synthesized samples and compared with the Pressure–Composition–Isotherm (PCI) of α-Li_3N compound at 255 °C. Phase composition for the hydrogenated samples at this two different H contents were studied by synchrotron powder diffraction. The results of the Rietveld analysis are gathered in Table 1 and typical refined diffraction pattern is shown in Fig. 4 for $Li_{2.55}Co_{0.04}N$ (Synchrotron diffraction refined composition) with $0.7H/Li_3N$. It is clear from Table 1 that for the same H concentrations, the hydrogenation reaction leads to different results depending on *M*. From previous *in situ* neutron diffraction, the formation of Li_4NH for H/Li_3N ~0.7 [16] was reported. In our study, the Li_4NH phase was indeed observed for Li_3N at H/Li_3N ~0.7, but not for the transition-metal doped samples $Li_{3-x}M_xN$.

Table 1
Molar phase fraction (%) derived from the refinement of the XRD data for the different samples at various H concentrations.

H/Li_3N	Phase	Mol %	Refined composition	Cell parameters (Å)	Cell volume (Å^3)	R_{Bragg}
$Li_3N + 5.5\%Ni$						
0	α-$Li_{3-x}Ni_xN$	92.1	$Li_{2.50(2)}Ni_{0.03(1)}N$	$a = 3.6713(1)$ $c = 3.8582(1)$	45.035(2)	0.16
	Li_2O	7.7	Li_2O	$a = 4.6277\ (3)$	99.10 (1)	0.42
	Ni	0.2	Ni	$a = 3.5239(1)$	43.759(2)	0.17
~0.7	α-$Li_{3-x}Ni_xN$	47.1	$Li_{2.50(2)}Ni_{0.03(1)}N$	$a = 3.6631(1)$ $c = 3.8583(1)$	44.834(1)	0.10
	Li_2O	10.0	Li_2O	$a = 4.6242$	98.88	0.04
	Ni	2.0	Ni	$a = 3.5233(1)$	43.759(2)	0.09
	Li_2NH	20.1	$Li_{1.7}NH_{1.3}$	$a = 5.0066(2)$	125.50(1)	0.04
	$Li_3N_2H_3$	6.7	$Li_{1.4}NH_{1.6}$	$a = 5.0485(3)$	128.68(1)	0.04
	LiH	13.3	LiH	$a = 4.0831(2)$	68.070(5)	0.14
	$Li_5Ni_3N_3$	0.8	$Li_5(Li_{0.4}Ni_{0.6})_3N_3$	$a = 6.4416(7)$ $c = 3.562(1)$	128.00(5)	0.18
~1.4	α- $Li_{3-x}Ni_xN$	14.5	$Li_{2.50(2)}Ni_{0.03(1)}N$	$a = 3.6701(1)$ $c = 3.8582(1)$	45.005(2)	0.11
	Li_2O	7.8	Li_2O	$a = 4.6242$	98.88	0.08
	Ni	3.1	Ni	$a = 3.52253(7)$	43.708(1)	0.09
	Li_2NH	39.1	$Li_{1.7}NH_{1.3}$	$a = 5.01123(6)$	125.844(3)	0.05
	$Li_3N_2H_3$	3.1	$Li_{1.4}NH_{1.6}$	$a = 5.0485(3)$	129.15(1)	0.07
	LiH	32.2	LiH	$a = 4.08282(5)$	68.058(2)	0.07
	$Li_5Ni_3N_3$	0.3	$Li_5(Li_{0.4}Ni_{0.6})_3N_3$	$a = 6.4559(8)$ $c = 3.552(1)$	128.22(6)	0.20
$Li_3N + 5.5\%Co$						
0	α-$Li_{3-x}Co_xN$	89.8	$Li_{2.55(1)}Co_{0.04(1)}N$	$a = 3.67154(2)$ $c = 3.85069(4)$	44.954(1)	0.09
	Li_2O	10.2	Li_2O	$a = 4.6272(1)$	99.071(6)	0.15
~0.7	α-$Li_{3-x}Co_xN$	58.4	$Li_{2.55(1)}Co_{0.04(1)}N$	$a = 3.67421(4)$ $c = 3.84850(6)$	44.994(1)	0.07
	Li_2O	8.0	Li_2O	$a = 4.6253(1)$	98.948(5)	0.09
	Li_2NH	9.2	Li_2NH	$a = 5.0065(4)$	125.49(2)	0.08
	$Li_3N_2H_3$	2.8	$Li_{1.4}NH_{1.6}$	$a = 5.0602(5)$	129.57(3)	0.13
	LiH	21.6	LiH	$a = 4.0833(3)$	68.08(1)	0.38
~1.4	α-$Li_{3-x}Co_xN$	16.7	$Li_{2.55(1)}Co_{0.04(1)}N$	$a = 3.6740(1)$ $c = 3.8473(2)$	44.974(3)	0.19
	Li_2O	4.7	Li_2O	$a = 4.6232(1)$	98.817(4)	0.11
	Li_2NH	34.7	$Li_{1.8}NH_{1.2}$	$a = 5.0182(1)$	126.367(5)	0.09
	LiH	43.9	LiH	$a = 4.08266(6)$	68.050(2)	0.20
$Li_3N + 11\%Co$						
0	α-$Li_{3-x}Co_xN$	90.1	$Li_{2.51(2)}Co_{0.09(1)}N$	$a = 3.67532(3)$ $c = 3.83469(6)$	44.859(1)	0.10
	Li_2O	8.7	Li_2O	$a = 4.6272(2)$	99.072(6)	0.11
	Co	0.6	Co	$a = 3.5428(2)$	44.465(4)	0.24
~0.7	α-$Li_{3-x}Co_xN$	40.1	$Li_{2.56(2)}Co_{0.11(1)}N$	$a = 3.68644(7)$ $c = 3.8297(2)$	45.073(3)	0.19
	Li_2O	6.9	Li_2O	$a = 4.6249(1)$	98.927(6)	0.07
	Co	0.4	Co	$a = 3.5428$	44.465	0.26
	Li_2NH	21.3	$Li_{1.8}NH_{1.2}$	$a = 5.0149(6)$	126.12(3)	0.12
	LiH	31.3	LiH	$a = 4.0825(3)$	68.044(8)	0.29
~1.4	α-$Li_{3-x}Co_xN$	4.8	$Li_{2.67(5)}Co_{0.11(1)}N$	$a = 3.6847(3)$ $c = 3.829(1)$	45.03(1)	0.45
	Li_2O	6.2	Li_2O	$a = 4.62275(7)$	98.788(3)	0.11
	Co	0.5	Co	$a = 3.5388(3)$	44.317(6)	0.44
	Li_2NH	43.9	$Li_{1.8}NH_{1.2}$	$a = 5.0210(1)$	126.581(5)	0.11
	LiH	44.6	LiH	$a = 4.08291(4)$	68.063(1)	0.12

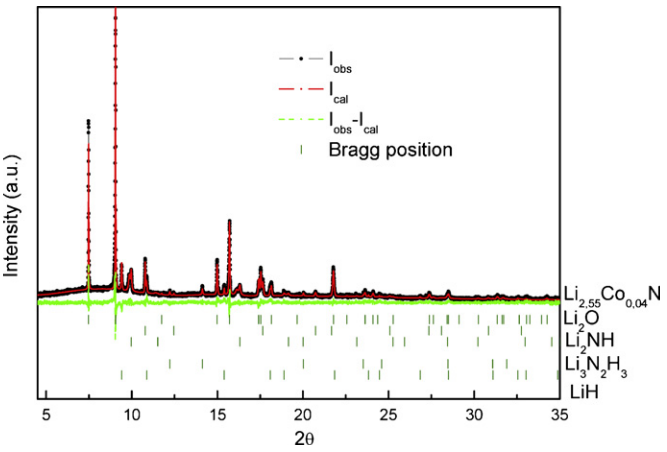

Fig. 4. Refined X-ray pattern of $Li_{2.55}Co_{0.04}N$ (Reitveld determined composition) with $0.7H/Li_3N$. obtained from synchrotron diffraction analysis (measured (dots), calculated (solid line), and difference curves (below); Vertical bars correspond to diffraction line positions of the phases).

The absence of the Li_4NH phase is not yet clearly understood but the reaction path with H_2 for $Li_{2.95}Ni_{0.05}N$ and $Li_{3-x}Co_xN$ ($x = 0.05$, 0.11) is obviously not the same. For Li_3N at low H concentration, the following reactions can be written:

$$3Li_3N + 2H_2 \rightarrow 2Li_2NH + Li_4NH + LiH \qquad (5)$$

$$Li_4NH + H_2 \rightarrow Li_2NH + 2LiH \qquad (6)$$

For $M = Ni$, with increasing H concentrations, the observed molar fraction of pure Ni metal increases from 0.2 to 3.1 at.%. The Ni precipitates may play a catalytic effect in the conversion of the compound, which can accelerate reaction (6). That may also imply that the metal substitution prevents reaction (7)

$$2Li(M)_3N + H_2 \rightarrow Li_2NH + Li(M)_4NH \qquad (7)$$

which is part of reaction (5) and/or that the $(Li,M)_4NH$ phase is not stable. Furthermore, a phase $Li_5Ni_3N_3$ [20] is formed. It suggests that the Ni-substituted Li_2NH imide phase is less stable than Ni metal and the $Li_5Ni_3N_3$ phase.

For $M = Co$, the $Li_{3-x}Co_xN$ compound does not show Co metal decomposition upon hydrogenation since metallic Co rate keeps constant to the amount observed just after the SPS treatment. Upon hydrogenation, $Li_{2.95}Co_{0.05}N$ and $Li_{2.89}Co_{0.11}N$ compounds transform into imide and LiH according to Eq. (1). The intermediate phase $Li_3N_2H_3$, which should be observed for H/Li_3N ~1.4, was not observed for the commercial sample Li_3N and $Li_{2.89}Co_{0.11}N$. In contrast, it is present at H/Li_3N = 0.7 and 1.4 for $Li_{2.95}Ni_{0.05}N$ and at H/Li_3N = 0.7 for $Li_{2.95}Co_{0.05}N$. Finally, for all samples, the quantity of LiH phase is well correlated to the Li_2NH phase amount.

4. Conclusion

The ternary phases $Li_{3-x}M_xN$ (M = Co or Ni) have been successfully prepared by SPS with 5 at.% (M = Co or Ni) and 10 at.% (M = Co). Those three compounds can be hydrogenated up to 0.7 and 1.4H/Li_3N at 255 °C under 10 bar of hydrogen. The formation of Li_4NH previously reported for Li_3N is not observed for transition metal doped samples $Li_{3-x}M_xN$. For M = Ni, the Ni atoms are released from the main phase upon hydrogenation and formation of Li_2NH, Li_3NH_3, LiH and $Li_5Ni_3N_3$ is observed. For M = Co, the Co atoms are not released upon hydrogenation and formation of Li_2NH, Li_3NH_3 and LiH phase is observed.

Acknowledgment

The authors wish to thank the SNBL beam line staff at ESRF, Grenoble (France) for help during the synchrotron data collection.

References

[1] F.W. Dafert, R. Miklauz, Monatsch. Chem. 31 (1910) 981–996, 30 (1909) 649-654.

[2] P. Chen, Z. Xiong, J. Luo, J. Lin, K.L. Tan, Nature 420 (2002) 302–304.

[3] T. Ichikawa, S. Isobe, N. Hanada, H. Fujii, J. Alloys Compd. 365 (2004) 271–276.

[4] Y. Kojima, Y. Kawai, J. Alloys Compd. 395 (2005) 236–239.

[5] T. Ichikawa, H.Y. Leng, S. Isobe, N. Hanada, H. Fujii, J. Power Sources 159 (2006) 126–131.

[6] W. Luo, J. Wang, K. Stewart, M. Clift, K. Gross, J. Alloys Compd. 446–447 (2007) 336–341.

[7] Y.H. Hu, N.Y. Yu, E. Ruckenstein, Ind. Eng. Chem. Res. 44 (2005) 4304–4309.

[8] M. Gupta, R.P. Gupta, J. Alloys Compd. 446–447 (2007) 319–322.

[9] J.B. Ducros, S. Bach, J.P. Pereira-Ramos, P. Willmann, Electrochim. Acta 52 (2007) 7035–7041.

[10] J.B. Ducros, S. Bach, J.P. Pereira-Ramos, P. Willmann, J. Power Sources 175 (2008) 517–525.

[11] A.G. Gordon, R.I. Smith, C. Wilson, Z. Stoeva, D.H. Gregory, Chem. Commun. (2004) 2812–2813.

[12] D.H. Gregory, Chem. Record 8 (2008) 229–239.

[13] S. Bach, J.P. Pereira-Ramos, J.B. Ducros, P. Willmann, Solid State Ionics 180 (2009) 231–235.

[14] D. Liu, F. Du, W. Pan, G. Chen, C. Wang, Y. Wei, Mater. Lett. 63 (2009) 504–506.

[15] L. Ma, P. Wang, H. Dai, L. Kong, H. Cheng, J. Alloys Compd. 466 (2008) L1–L4.

[16] E. Weidner, D.J. Bull, I.L. Shabalin, S.G. Keens, M.T.F. Telling, D.K. Ross, Chem. Phys. Lett. 444 (2007) 76–79.

[17] W.I.F. David, M.O. Jones, D.H. Gregory, C.M. Jewell, S.R. Johnson, A. Walton, P.P. Edwards, J. Am. Chem. Soc. 129 (2007) 1594–1601.

[18] J.-C. Crivello, M. Gupta, R. Černý, M. Latroche, D. Chandra, Phys. Rev. B 81 (2010) 104113–104211.

[19] J. Rodríguez-Carvajal, Physica B. 26 (2001) 12–19;
J. Rodríguez-Carvajal, Newsletter Comm Powder Diffraction (IUCr) 192 (1993) 55–69.

[20] J. Klatyk, P. Höhn, R. Kniep, Z. Kristallogr, New Crystal Struct. (1998) 213–231.